Supplementary Information

A Novel 2D Eu-MOF as a Dual-Functional Fluorescence Sensor for Detection of benzaldehyde and Fe^{3+}

Xiaole Wang[a] and Weisheng Liu*[a]

[a] Key Laboratory of Nonferrous Metals Chemistry and Resources Utilization of Gansu Province, State Key Laboratory of Applied Organic Chemistry and College of Chemistry and Chemical Engineering, Lanzhou University, 730000, Lanzhou, China. E-mail: liuws@lzu.edu.cn.

Materials and instruments:

All solvents and reagents were commercially available A.R. grade and used without further purification. Powder X-ray diffraction data were obtained by using a PAN type X'Pert Pro diffractometer operated at 40 kV and 40 mA with Cu Kα radiation. The FT-IR spectra were recorded from KBr pellets in the range from 4000 to 500 cm^{-1} on a Bruker VERTEX 70 spectrometer, and the UV-visible spectrum was measured by the UV-2700 UV-VIS Spectrophotometer. Thermogravimetric analyses were obtained on a NETZSCH STA 449 F3 Jupiter® under a N_2 atmosphere. The luminescence spectrum was measured by the Hitachi T-7000FL fluorescence spectrometer.

X-ray Structural Crystallography:

Single-crystal X-ray diffraction data were collected on Agilent Super Nova Single Crystal Diffractometer equipped with graphite-monochromatic Mo-Kα source (λ=0.71073 Å). The crystal was kept at 150.00(11) K during data collection. Using Olex2[1], the structure was solved with the SHELXT[2] structure solution program using Intrinsic Phasing and refined with the SHELXL[3] refinement package using Least Squares minimization.

Synthesis of ligand：

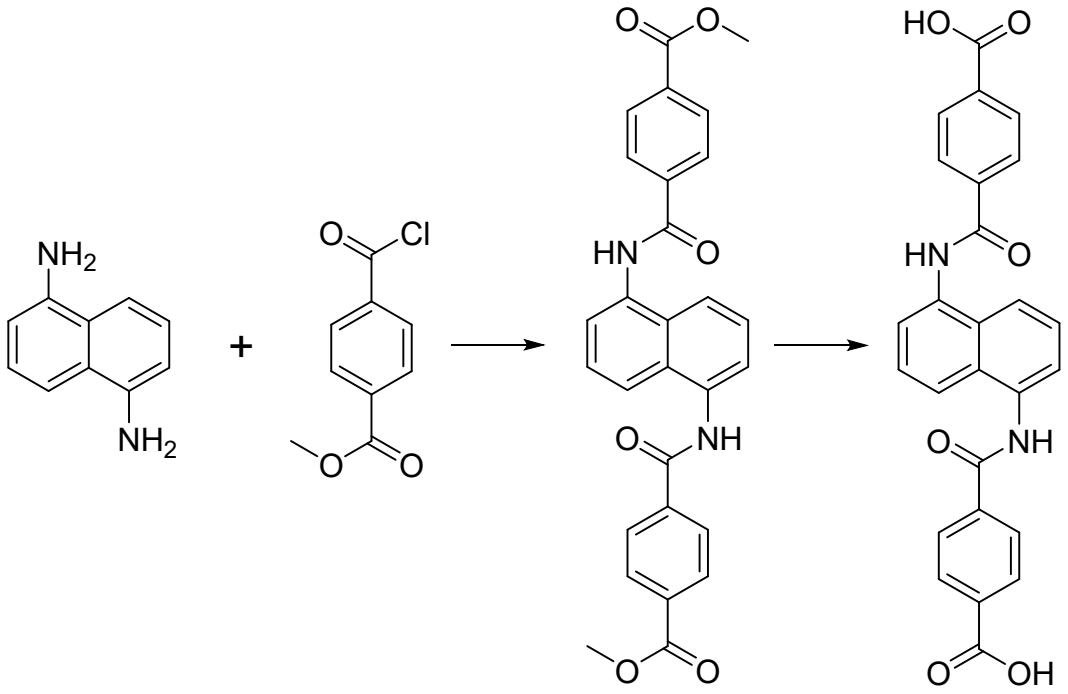

Scheme S1. Synthesis of ligand.

Methyl 4-(chlorocarbonyl)benzoate (2.67 g, 13.44 mmol) was dispersed with 1,5-diaminonaphthalene (1.028 g, 6.5 mmol) in dichloromethane (100 mL) under stirring conditions. The reaction system was placed in an ice bath and allowed to cool to 0 °C. Triethylamine (2 ml, excess) was added dropwise to the mixture using a constant pressure funnel and stirred, after which the ice bath was removed and the mixture was allowed to continue stirring at room temperature for one hour. The system was then heated to reflux for 48 h. A large amount of grey solid was observed. At the end of the reaction, the solvent was removed by distillation under reduced pressure and washed with dilute hydrochloric acid, water, saturated sodium bicarbonate solution, and water, respectively, and dried to obtain a grey solid powder. The solid obtained in the previous step of the reaction was added to 80 mL of a methanol-water mixture (methanol: water = 5: 1) of potassium hydroxide (1.122 g, 20 mmol) and stirred at reflux with heating at 90 °C for 36 h. Gradual dissolution of the solid was observed to give a dark-coloured clarified solution. After the solution was concentrated to about 20 ml by reduced

pressure distillation, its pH was adjusted to 3 by adding dilute hydrochloric acid, and a large amount of grey solid was precipitated, which was filtered, washed and dried to obtain the solid powder H_2L (4,4'-((naphthalene-1,5-diylbis(azanediyl))bis(carbonyl)) dibenzoic acid) (2.54 g, yield: 86%).

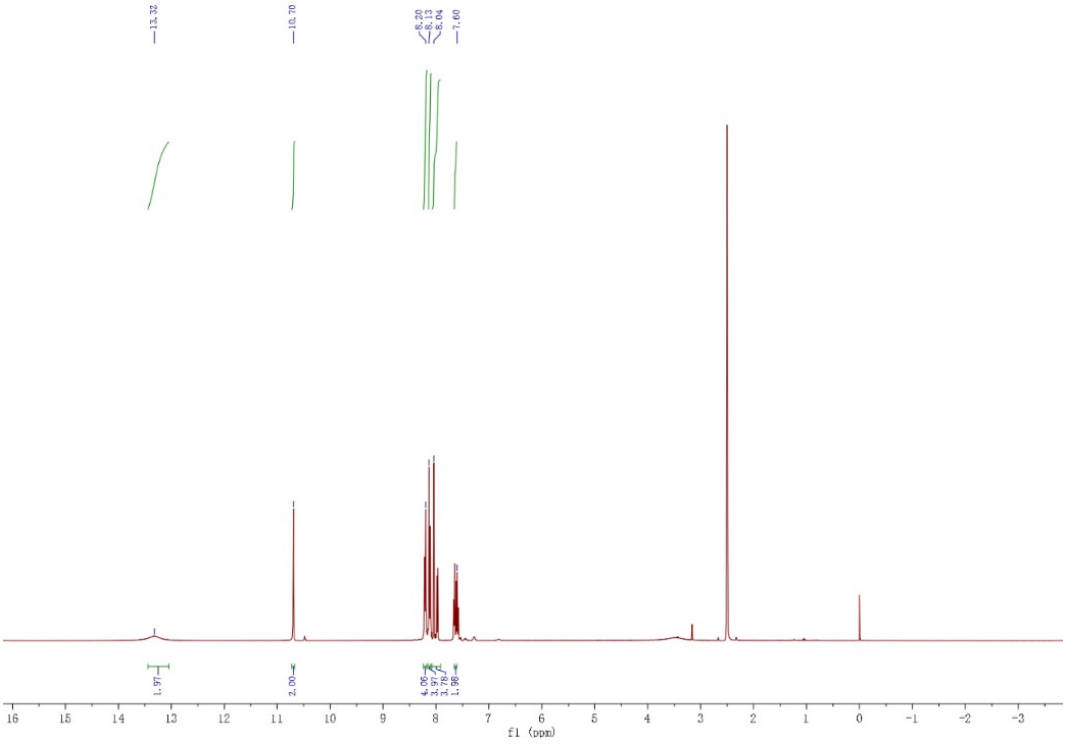

Figure S1. (a) ^{1}H NMR spectra of Ligand (DMSO-d_6, 400MHz).

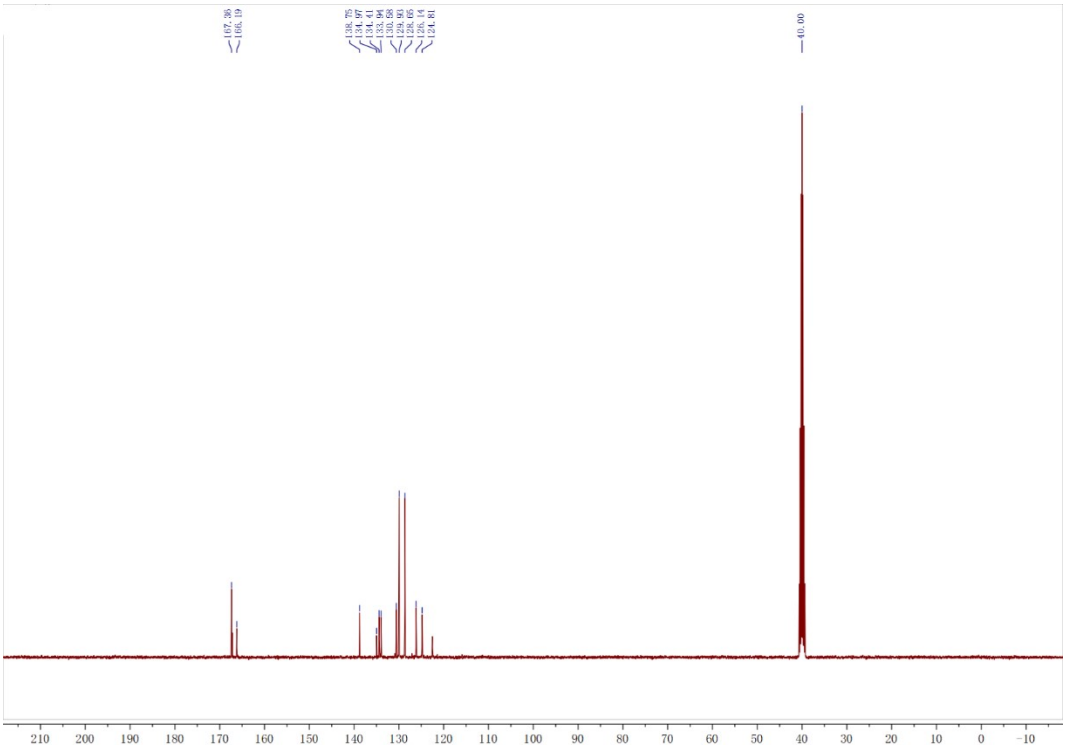

Figure S1. (b) ^{13}C NMR spectra of Ligand (DMSO-d_6, 101MHz).

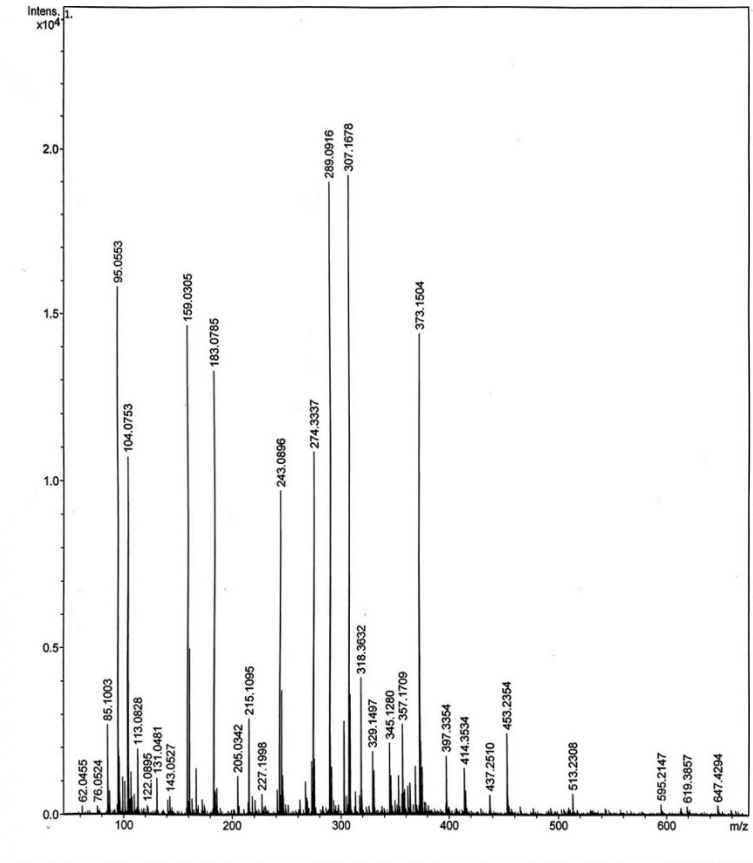

Figure S1. (c) Mass spectra of Ligand.

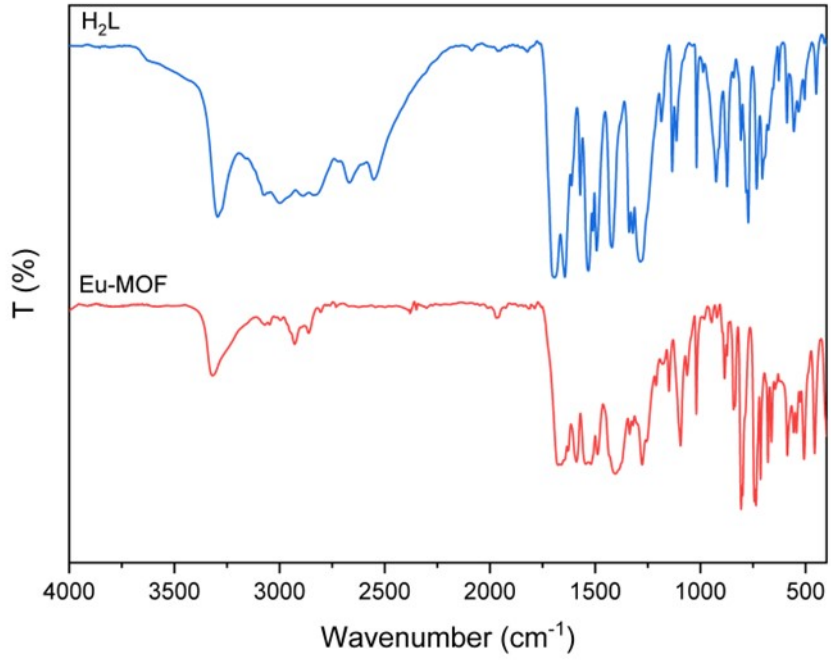

Figure S2. FT-IR spectra of the Eu-MOF and ligand.

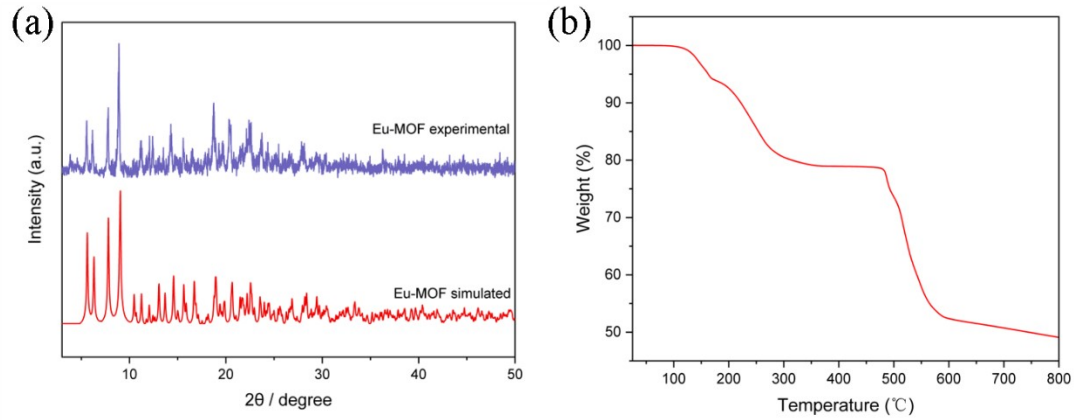

Figure S3. (a) The PXRD patterns of Eu-MOF. (b) TGA plot of the Eu-MOF.

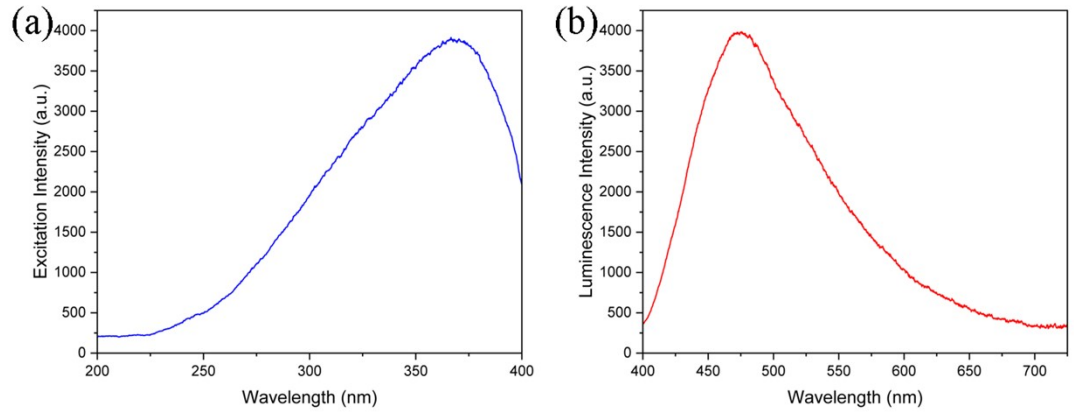

Figure S4. (a) The solid-state excitation spectrum of H_2L at room temperature (λ_{em} = 473 nm). (b) The solid-state emission spectrum of H_2L at room temperature (λ_{ex} = 367 nm).

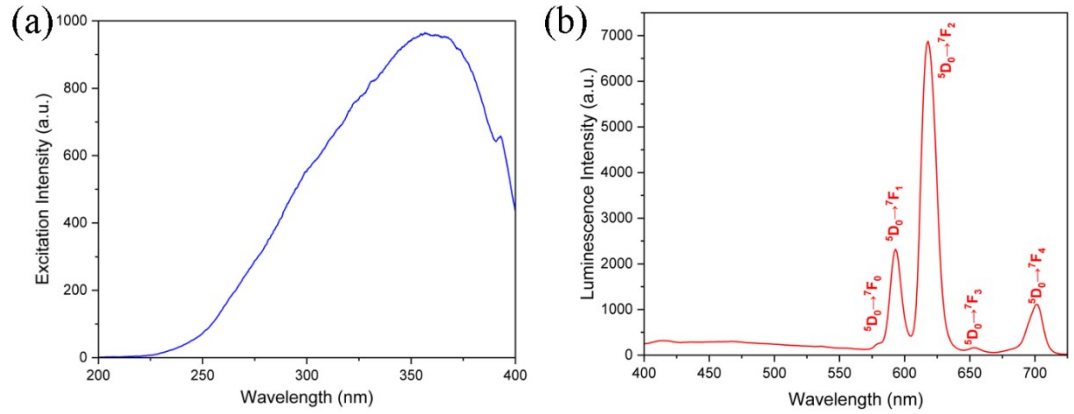

Figure S5. (a) The solid-state excitation spectrum of Eu-MOF at room temperature (λ_{em} = 618 nm). (b) The solid-state emission spectrum of Eu-MOF at room temperature (λ_{ex} = 367 nm).

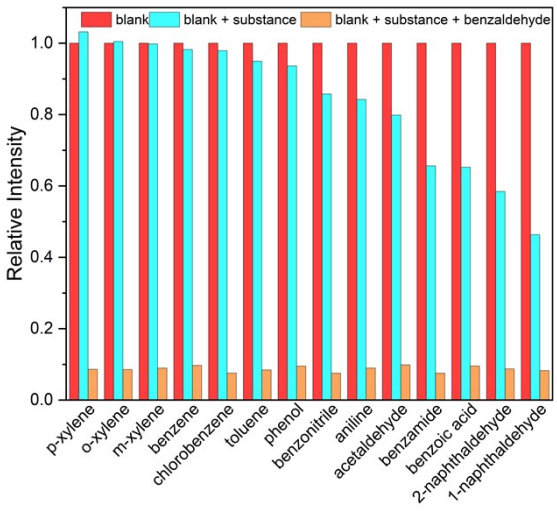

Figure S6. The relative luminous intensity of Eu-MOF dispersed in various solutions with and without benzaldehyde.

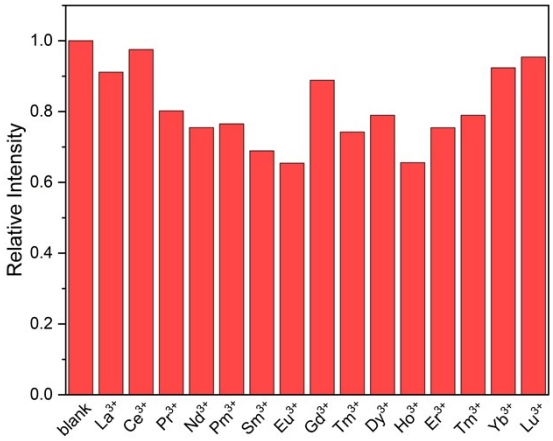

Figure S7. Comparison of the luminescence intensity at 618 nm for systems incorporating different lanthanide ions.

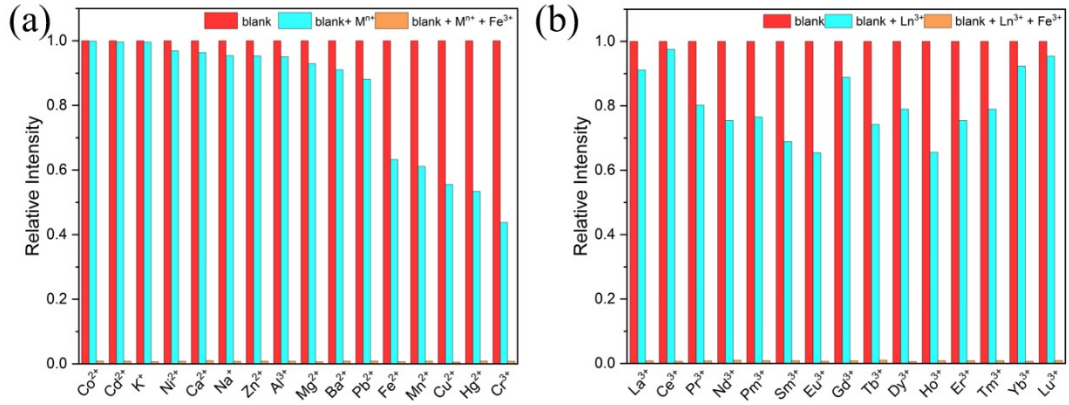

Figure S8. The relative luminous intensity of Eu-MOF dispersed in various solutions with and without Fe^{3+}.

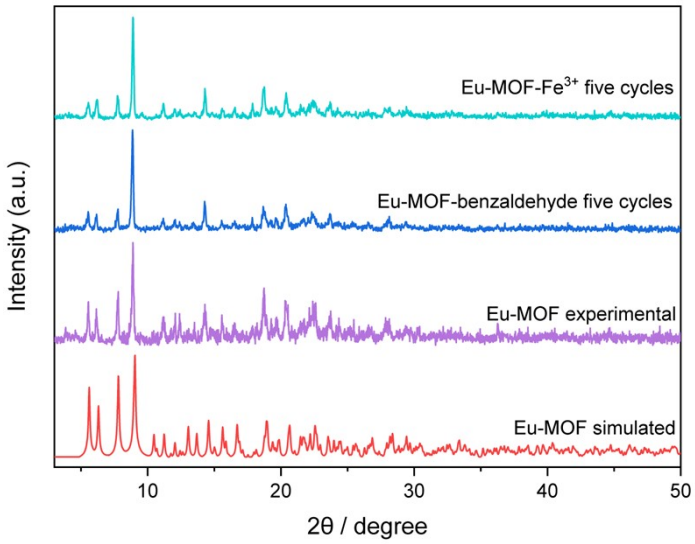

Figure S9. The PXRD patterns of Eu-MOF and Eu-MOF after five cycles experiment for the detection of benzaldehyde and Fe^{3+}.

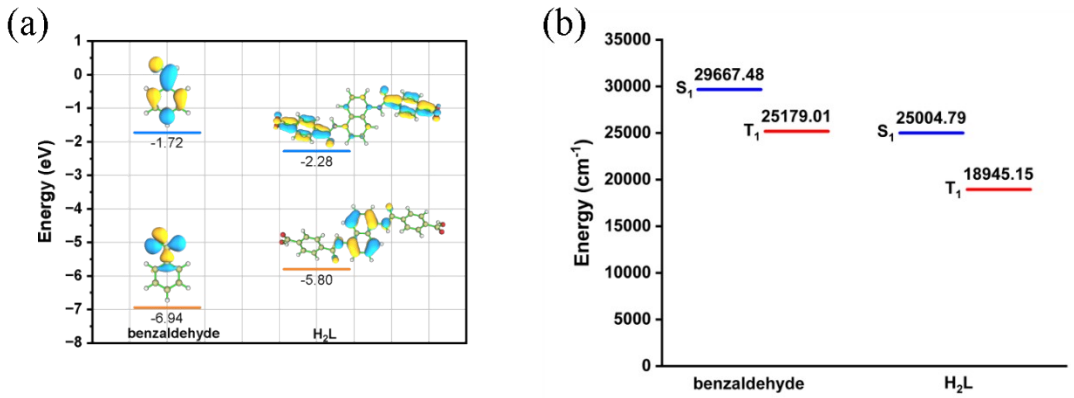

Figure S10. (a) LUMO and HOMO energy levels of benzaldehyde and ligand calculated by the DFT at the B3LYP/6-31 G level. (b) S1 and T1 energy levels of benzaldehyde and ligand.

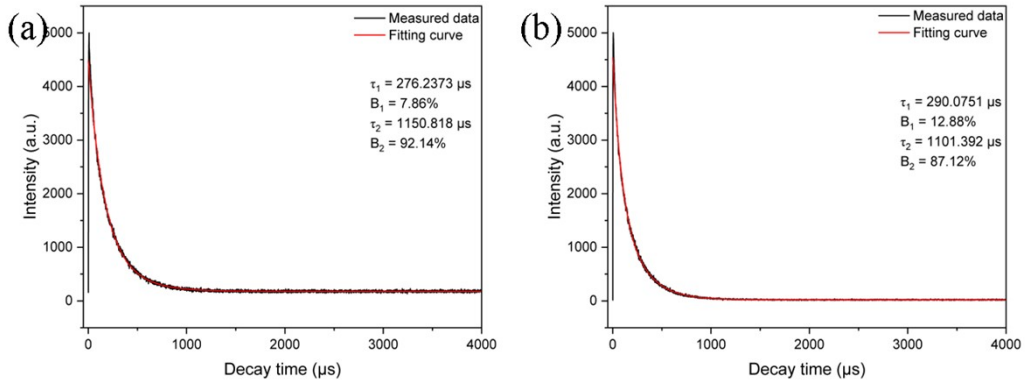

Figure S11. (a) Fluorescence lifetime of Eu-MOF measured in benzyl alcohol. (b) Fluorescence lifetime of Eu-MOF after addition of benzaldehyde.

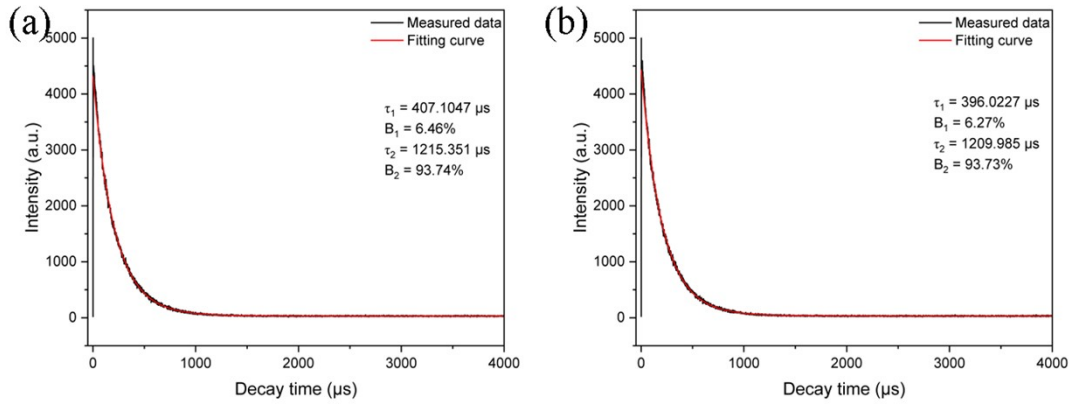

Figure S12. (a) Fluorescence lifetime of Eu-MOF measured in DMF; (b) Fluorescence lifetime of Eu-MOF after Fe^{3+} addition.

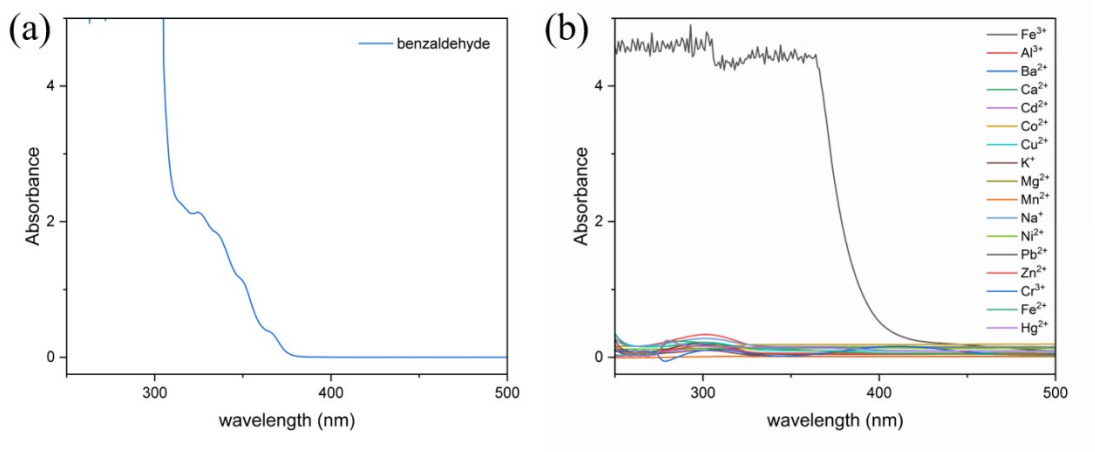

Figure S13. Ultraviolet-visible absorption spectra of (a) benzaldehyde and (b) various metal cations.

Table S1. Performance of fluorescent sensors for the detection of benzaldehyde.

Sensor	Analyte	Ksv (M^{-1})	LOD (M)	Ref
Eu-MOF	Benzaldehyde	2283	9.3×10^{-6}	This work
$[Zn_2(DPA)(OBA)_2].2DMF \cdot 4H_2O$	Benzaldehyde	27.79	3.8×10^{-3}	4
ANDP	Benzaldehyde	1505	3.98×10^{-5}	5
$[Ni(5\text{-}NIP)(L)(H_2O)]_n$	Benzaldehyde	3881	5.86×10^{-5}	6
$[Ni(1,4\text{-}PDA)(L)(H_2O)_n$	Benzaldehyde	2162	7.32×10^{-5}	6
$[Co(OBA)(L1)_{0.5}]_n$	Benzaldehyde	1097	2.23×10^{-6}	9
$[Eu(L)(HCOO)(H_2O)]_n$	Benzaldehyde	1295	1.1×10^{-6}	12
$[Tb(L)(HCOO)(H_2O)]_n$	Benzaldehyde	989	1.9×10^{-6}	12
$[Tb(bidc)(Hbidc)(H_2O)]_n$	Benzaldehyde	734	1.44×10^{-4}	14
$[Tb_3(bidc)_4(HCOO)(DMF)]_n$	Benzaldehyde	3664	1.35×10^{-5}	14
$[\{Eu(SIP)(H_2O)_4\}]_n$	Benzaldehyde	9800	1×10^{-6}	15

Table S2. Performance of MOF-based fluorescent sensors for the detection of Fe^{3+}.

Sensor	Analyte	Ksv (M^{-1})	LOD (M)	Ref
Eu-MOF	Fe^{3+}	3656	5.8×10^{-6}	This work
$[Ni(5\text{-}NIP)(L)(H_2O)]_n$	Fe^{3+}	1651	6.57×10^{-5}	6
$[Ni(1,4\text{-}PDA)(L)(H_2O)_n$	Fe^{3+}	2810	5.85×10^{-5}	6
$[Cd_{0.5}(TBTA)_{0.5}(L1)]_n$	Fe^{3+}	6186	2.645×10^{-5}	7
534-MOF-Tb	Fe^{3+}	5510	0.13×10^{-3}	8
$[Co(OBA)(L1)_{0.5}]_n$	Fe^{3+}	3540	6.92×10^{-5}	9
$[Co(HBTC)(L2)]_n$	Fe^{3+}	1970	1.016×10^{-5}	9
1-Eu	Fe^{3+}	5300	1.16×10^{-3}	10
[Zn(PrOip)(bpp)(H2O)]n	Fe3+	4404	6.676×10^{-5}	11
{[Zn(nBuOip)(bpp)]·2H2O}n	Fe3+	1474	5.442×10^{-5}	11
$\{[Zn(^{i}BuOip)(bpp)]\cdot 2H_2O\}_n$	Fe^{3+}	1714	1.773×10^{-5}	11
$[Zn(p\text{-}CNPhHIDC)(4,4'\text{-}bipy)]_n$	Fe^{3+}	1370	5×10^{-3}	13
[Cd(p-CNPhHIDC)(4,4'-bipy)0.5]$_n$	Fe^{3+}	1990	5×10^{-3}	13

References

1. Dolomanov, O.V., Bourhis, L.J., Gildea, R.J, Howard, J.A.K. & Puschmann, H. (2009). *J. Appl. Cryst.*, **42**, 339-341.

2. Sheldrick, G.M. (2015). *Acta Cryst.* **A71**, 3-8.

3. Sheldrick, G.M. (2015). *Acta Cryst.* **C71**, 3-8.

4. S.M. Zhao, Z.F. Qiu, Z.H. Xu, Z.Q. Huang, Y. Zhao, W.Y. Sun, (2022). *Dalt. Trans.*, **51**, 3572–3580,

5. Verma, T., Verma, P., & Singh, U. P. (2023). *Microchem. J*, **191**, 108771.

6. K. Lyu, Y. Wei, Y. Li, G. Cui, (2021). *J. Mol. Struct.* **1225**, 129128–129138.

7. Liu, Y., Han, C., & Cui, G. H.(2021). *Inorg. Chim. Acta.*, **525**, 120499.

8. Chen, M., Xu, W. M., Tian, J. Y., Cui, H., Zhang, J. X., Liu, C. S., & Du, M. (2017). *J. Mater. Chem. C*, **5**, 2015-2021.

9. Liu, Y., Ren, L., & Cui, G. H. (2021). *CrystEngComm*, **23**, 7485-7495.

10. Tong, W. Q., Liu, T. T., Li, G. P., Liang, J. Y., Hou, L., & Wang, Y. Y. (2018). *New J. Chem*, **42**, 9221-9227.

11. Zhu, R. R., Wang, T., Wang, D. W., Yan, T., Wang, Q., Li, H. X. & Zhao, Q. H. (2019). *New J. Chem*, **43**, 1494-1504.

12. Sun, Z., Yang, M., Ma, Y., & Li, L. (2017). *Cryst Growth Des*, **17**, 4326-4335.

13. Zhang, J., Zhao, L., Liu, Y., Li, M., Li, G. & Meng, X. (2018). *New J. Chem*, **42**, 6839-6847.

14. Wang, L., He, Q. Q., Gao, Q., Xu, H., Zheng, T. F., Zhu, Z. H. & Wen, H. R. (2023). *Inorg. Chem*, **62**, 3799-3807.

15. Che, X. J., Hou, S. L., Shi, Y., Yang, G. L., Hou, Y. L. & Zhao, B. (2019). *Dalt. Trans.*, **48**, 3453-3458.

Table S3. Crystal data and structure refinement for the Eu-MOF.

CCDC	2337133
Empirical formula	$C_{42}H_{31}EuN_4O_{10}$
Formula weight	903.67
Temperature/K	150.00(11)
Crystal system	triclinic
Space group	P-1
a/Å	9.87340(10)
b/Å	14.1754(2)
c/Å	15.9145(2)
α/°	98.4420(10)
β/°	90.8970(10)
γ/°	92.6890(10)
Volume/Å^3	2200.25(5)
Z	2
ρ_{calc}g/cm^3	1.364
μ/mm^{-1}	1.482
F(000)	908.0
Crystal size/mm^3	0.07 × 0.06 × 0.04
Radiation	Mo Kα (λ = 0.71073)
2Θ range for data collection/°	4.924 to 62.182
Index ranges	$-12 \le h \le 13$, $-20 \le k \le 20$, $-22 \le l \le 22$
Reflections collected	70486
Independent reflections	12054 [R_{int} = 0.0691, R_{sigma} = 0.0525]

Data/restraints/parameters	12054/13/525
Goodness-of-fit on F^2	1.042
Final R indexes [I>=2σ (I)]	$R_1 = 0.0296$, $wR_2 = 0.0585$
Final R indexes [all data]	$R_1 = 0.0370$, $wR_2 = 0.0613$
Largest diff. peak/hole / e $Å^{-3}$	1.49/-0.61

Table S4. Bond Lengths for the Eu-MOF.

Atom	Atom	Length/Å	Atom	Atom	Length/Å
Eu1	Eu11	4.30922(17)	C4	C10	1.505(3)
Eu1	O11	2.4175(14)	C5	C19	1.374(3)
Eu1	O3	2.3825(16)	C5	C39	1.400(3)
Eu1	O4	2.3144(13)	C6	C16	1.380(3)
Eu1	O62	2.3509(14)	C6	C24	1.389(3)
Eu1	O8	2.3159(13)	C7	C39	1.370(3)
Eu1	O103	2.3627(13)	C7	C42	1.414(3)
Eu1	O114	2.3725(13)	C8	C14	1.509(3)
Eu1	C11	3.1779(19)	C10	C12	1.388(3)
O1	C1	1.262(2)	C10	C20	1.388(3)
O2	C37	1.214(3)	C11	C21	1.410(3)
O3	C36	1.230(3)	C11	C30	1.364(3)
O4	C8	1.259(2)	C12	C22	1.389(3)
O5	C33	1.255(4)	C13	C16	1.391(3)
O6	C4	1.263(2)	C13	C32	1.391(3)
O7	C27	1.235(3)	C14	C18	1.389(3)
O8	C1	1.261(2)	C14	C38	1.385(3)
O9	C33	1.297(6)	C15	C20	1.386(3)
O10	C8	1.252(2)	C15	C26	1.391(3)
O11	C4	1.258(2)	C17	C29	1.371(3)

Atom	Atom	Length/Å	Atom	Atom	Length/Å
N1	C30	1.428(2)	C18	C40	1.381(3)
N1	C33	1.330(3)	C19	C34	1.424(3)
N2	C19	1.423(3)	C21	C23	1.365(3)
N2	C27	1.348(3)	C22	C26	1.386(3)
N3	C25	1.441(3)	C23	C34	1.419(3)
N3	C37	1.345(3)	C24	C31	1.381(3)
N4	C9	1.446(3)	C25	C28	1.421(3)
N4	C36	1.323(3)	C26	C27	1.495(3)
N4	C41	1.467(3)	C28	C285	1.422(4)
C1	C6	1.505(3)	C28	C295	1.421(3)
C2	C17	1.407(3)	C30	C42	1.426(3)
C2	C25	1.358(3)	C31	C32	1.393(3)
C3	C35	1.392(3)	C32	C33	1.507(3)
C3	C37	1.508(3)	C34	C42	1.433(3)
C3	C40	1.392(3)	C35	C38	1.392(3)

[1]1-X,-Y,1-Z; [2]1-X,1-Y,-Z; [3]-X,-Y,1-Z; [4]+X,-1+Y,1+Z; [5]-X,-1-Y,2-Z

Table S3. Bond Angles for the Eu-MOF.

Atom	Atom	Atom	Angle/°	Atom	Atom	Atom	Angle/°
O1[1]	Eu1	Eu1[1]	73.99(3)	C24	C6	C1	119.94(18)
O1[1]	Eu1	C1[1]	20.93(5)	C39	C7	C42	120.33(19)
O3	Eu1	Eu1[1]	118.39(4)	O4	C8	C14	117.34(16)
O3	Eu1	O1[1]	133.08(5)	O10	C8	O4	125.80(18)
O3	Eu1	C1[1]	132.53(5)	O10	C8	C14	116.85(17)
O4	Eu1	Eu1[1]	149.74(3)	C12	C10	C4	121.51(18)
O4	Eu1	O1[1]	76.43(5)	C12	C10	C20	119.52(19)
O4	Eu1	O3	78.41(5)	C20	C10	C4	118.81(18)
O4	Eu1	O6[2]	115.52(5)	C30	C11	C21	120.3(2)
O4	Eu1	O8	158.85(5)	C10	C12	C22	119.70(19)
O4	Eu1	O10[3]	80.50(5)	C32	C13	C16	119.99(19)
O4	Eu1	O11[4]	103.78(5)	C18	C14	C8	120.36(18)
O4	Eu1	C1[1]	95.88(5)	C38	C14	C8	120.16(17)
O6[2]	Eu1	Eu1[1]	64.49(3)	C38	C14	C18	119.48(18)
O6[2]	Eu1	O1[1]	78.74(5)	C20	C15	C26	119.6(2)
O6[2]	Eu1	O3	148.18(5)	C6	C16	C13	121.04(19)
O6[2]	Eu1	O10[3]	77.13(5)	C29	C17	C2	120.7(2)
O6[2]	Eu1	O11[4]	124.20(5)	C40	C18	C14	120.08(19)
O6[2]	Eu1	C1[1]	76.70(5)	N2	C19	C34	119.77(19)
O8	Eu1	Eu1[1]	50.15(3)	C5	C19	N2	119.5(2)

Atom	Atom	Atom	Angle/°	Atom	Atom	Atom	Angle/°
O8	Eu1	O1[1]	124.13(5)	C5	C19	C34	120.74(19)
O8	Eu1	O3	82.71(5)	C15	C20	C10	120.8(2)
O8	Eu1	O6[2]	76.86(5)	C23	C21	C11	120.7(2)
O8	Eu1	O10[3]	86.17(5)	C26	C22	C12	120.73(19)
O8	Eu1	O11[4]	80.11(5)	C21	C23	C34	120.63(19)
O8	Eu1	C11	103.93(5)	C31	C24	C6	120.2(2)
O10[3]	Eu1	Eu1[1]	125.92(3)	C2	C25	N3	120.66(19)
O10[3]	Eu1	O1[1]	134.92(5)	C2	C25	C28	121.52(19)
O10[3]	Eu1	O3	77.40(5)	C28	C25	N3	117.78(18)
O10[3]	Eu1	O11[4]	150.29(5)	C15	C26	C27	121.6(2)
O10[3]	Eu1	C1[1]	148.85(5)	C22	C26	C15	119.54(19)
O11[4]	Eu1	Eu1[1]	61.68(3)	C22	C26	C27	118.69(19)
O11[4]	Eu1	O1[1]	73.65(5)	O7	C27	N2	123.6(2)
O11[4]	Eu1	O3	74.81(5)	O7	C27	C26	120.39(19)
O11[4]	Eu1	C1[1]	60.75(5)	N2	C27	C26	116.01(18)
C11	Eu1	Eu1[1]	53.97(3)	C25	C28	C28[6]	118.4(2)
C1	O1	Eu1[1]	115.88(12)	C29[6]	C28	C25	122.68(18)
C36	O3	Eu1	141.11(14)	C29[6]	C28	C28[6]	118.9(2)
C8	O4	Eu1	143.65(14)	C17	C29	C28[6]	120.48(19)
C4	O6	Eu1[2]	132.34(13)	C11	C30	N1	119.87(19)

Atom	Atom	Atom	Angle/°	Atom	Atom	Atom	Angle/°
C1	O8	Eu1	163.79(14)	C11	C30	C42	121.16(18)
C8	O10	Eu1[3]	148.02(13)	C42	C30	N1	118.92(18)
C4	O11	Eu1[5]	143.20(13)	C24	C31	C32	121.0(2)
C33	N1	C30	123.06(17)	C13	C32	C31	118.62(19)
C27	N2	C19	123.57(18)	C13	C32	C33	123.87(19)
C37	N3	C25	120.79(17)	C31	C32	C33	117.45(19)
C9	N4	C41	117.3(2)	O5	C33	N1	120.8(2)
C36	N4	C9	120.6(2)	O5	C33	C32	120.5(2)
C36	N4	C41	122.2(2)	O9	C33	N1	119.3(3)
O1	C1	Eu1[1]	43.19(9)	O9	C33	C32	117.2(3)
O1	C1	C6	117.97(17)	N1	C33	C32	117.35(19)
O8	C1	Eu1[1]	86.10(11)	C19	C34	C42	117.93(19)
O8	C1	O1	123.95(18)	C23	C34	C19	122.95(19)
O8	C1	C6	117.98(16)	C23	C34	C42	119.09(19)
C6	C1	Eu1[1]	145.51(13)	C3	C35	C38	120.4(2)
C25	C2	C17	120.0(2)	O3	C36	N4	123.7(2)
C35	C3	C37	124.43(19)	O2	C37	N3	122.3(2)
C35	C3	C40	118.59(19)	O2	C37	C3	120.5(2)
C40	C3	C37	116.98(18)	N3	C37	C3	117.27(18)
O6	C4	C10	117.38(17)	C14	C38	C35	120.35(19)

Atom	Atom	Atom	Angle/°	Atom	Atom	Atom	Angle/°
O11	C4	O6	125.66(18)	C7	C39	C5	120.7(2)
O11	C4	C10	116.94(17)	C18	C40	C3	121.04(19)
C19	C5	C39	120.6(2)	C7	C42	C30	122.20(18)
C16	C6	C1	120.73(17)	C7	C42	C34	119.60(19)
C16	C6	C24	119.06(19)	C30	C42	C34	118.11(18)

[1]1-X,-Y,1-Z; [2]1-X,1-Y,-Z; [3]-X,-Y,1-Z; [4]+X,-1+Y,1+Z; [5]+X,1+Y,-1+Z; [6]-X,-1-Y,2-Z